buildings

MDPI

Article

Passive Night Cooling Potential in Office Buildings in Continental and Mediterranean Climate Zone in Croatia

Zoran Veršić , Marin Binički * and Mateja Nosil Mešić

Faculty of Architecture, University of Zagreb, 10000 Zagreb, Croatia
* Correspondence: marin.binicki@arhitekt.hr

Abstract: The envelope is one of the most important driving factors in the energy efficiency of buildings. Typical for office and commercial buildings, curtain wall facades allow solar heat gains to be used during the winter but can lead to difficulties in reducing the cooling load during summer. The cooling load is dominant in most building types in the temperate maritime climate, while in the temperate continental climate, it is dominant mainly in office and commercial buildings. The goal of this research was to determine the potential of night passive cooling in an office building model in the most populated urban areas in Croatia-Zagreb and Split, which are located in two different climate zones. Suitable to the climate on-site, an appropriate building envelope and various types of passive and mechanical ventilation systems were selected for each location and case. Additional factors included and analysed were climate conditions, heat gains, the heat accumulation of the building, night ventilation through openings, unwanted air infiltration, and cooling loads. Through a detailed description of the model, passive cooling potential calculations, and Computer Fluid Dynamics (CFD) simulations, the results showed a potential of up to 43.5% savings in the cooling energy need for the temperate continental climate and 32.2% in the temperate marine climate. It was found from the analysis that night ventilation is expected to cool down the building enough to delay a need for cooling by several hours and improve fresh air requirements, thus saving power for cooling, and effectively reducing the need for air conditioning.

Keywords: cross ventilation; cooling energy need; night ventilation cooling; passive cooling

check for updates

Citation: Veršić, Z.; Binički, M.; Nosil Mešić, M. Passive Night Cooling Potential in Office Buildings in Continental and Mediterranean Climate Zone in Croatia. *Buildings* **2022**, *12*, 1207. https://doi.org/10.3390/buildings12081207

Academic Editor: Danny Hin Wa Li

Received: 18 June 2022
Accepted: 3 August 2022
Published: 10 August 2022

1. Introduction

The climate in Croatia is unique since two different climate zones meet in a small area distinctly separated by a coastal mountain range. The continental climate zone in the northern, north-western, and eastern parts of the country is specific to central Europe, while the coastal climate zone, in Istria, the Kvarner Gulf, and Dalmatia, corresponds to the whole Mediterranean maritime climate (Veršić et al., 2018) [1].

Zagreb (45°48′ N; 15°58′ E) is located in the continental climate zone, a moderately warm and humid climate zone with hot summers, where summer peaks reach 33–36 °C, while Split (43°30′ N; 16°26′ E) is in the Mediterranean maritime climate zone, which is characterised by hot dry summers and cool, rainy winters, with summer peaks also ranging from 33 to 36 °C [2]. While summers are of similar temperatures in both climates, maritime climate winters are mild and continental winters are cold. In the continental climate, both winters and summers are challenging with regard to energy efficiency, while in the maritime climate, the focus is only on the cooling season.

The strategy of passive cooling through nightly air fluctuation is preferable for hot dry climate regions where day- and night-time temperatures differ minimally by 8 °C, with air speeds of at least 1.5 m/s. Ideal regions are arid climate zones, where the diurnal temperature range reaches 15 °C [2–4]. Examples of peak summer temperatures in July compared to night-before temperatures are represented in Figure 1 for both Zagreb (Meteorological dataset for Zagreb Grič) and Split (Meteorological dataset for Split Marjan).

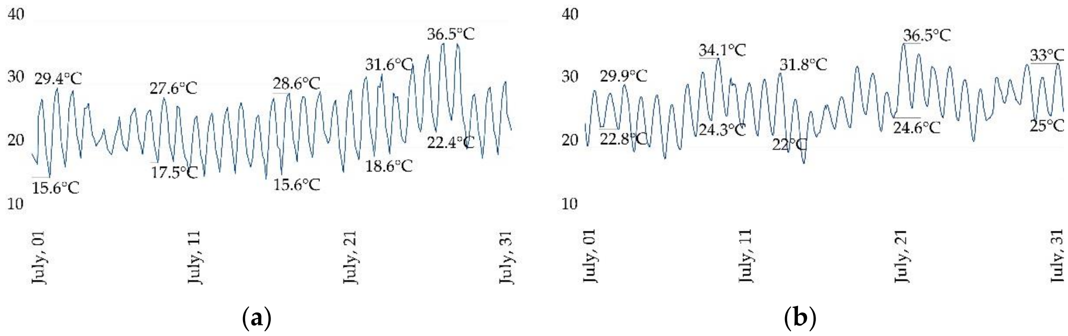

Figure 1. Daily temperatures in July in (**a**) Zagreb and (**b**) Split. All data was taken from typical meteorogical year based on years 2005−2020 [5].

According to meteorological datasets for the calculation of the energy performance of buildings prescribed by the European Commission (PVGIS [(c)] European Union, 2001–2022 climate dataset) [5], the average temperature between 8:00 pm and 7:00 am during the cooling period is 14.0 °C in Zagreb and 18.8 °C in Split. Considering the internal cooling temperature is set to 26 °C in both climates, the differences of 12 °C and 7.2 °C between the internal cooling temperature and the outer night temperatures show the potential for passive cooling.

As seen in the examples shown in Figure 2, for five days in July, according to PV GIS, the average annual wind speed is 2.47 m/s in Zagreb and 3.77 m/s in Split. The average night windspeed between 8:00 pm and 7:00 am during a cooling period is 2.17 m/s in Zagreb and 3.21 m/s in Split [5]. The reason for the higher windspeed values in the Mediterranean climate is that coastal breezes change their day and night directions, supporting nocturnal ventilation on the land side [6].

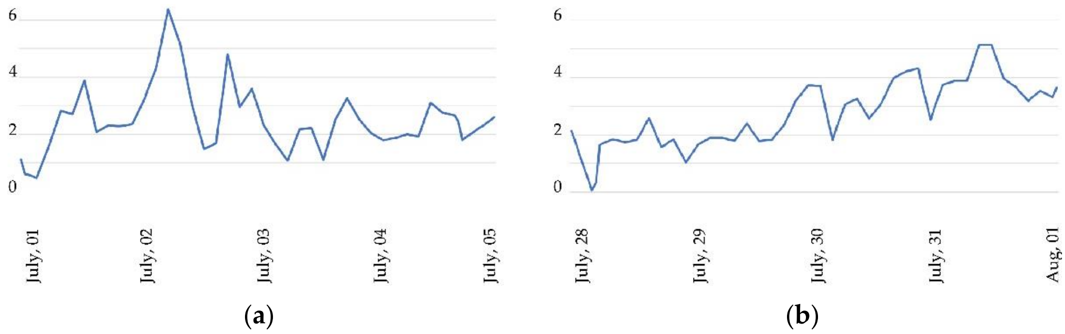

Figure 2. Wind speed in m/s (**a**) from 1–5 July, Zagreb; (**b**) from 28 July–1 August, Split. All data was taken from typical meteorogical year based on years 2005−2020 [5].

There are many methods of passive cooling that can be applied to both existing and newly omnipresent, low-energy buildings. Some of the traditional approaches include stack ventilation, cooling towers, solar chimneys, evaporative cooling, and solar control (obtained by, e.g., room orientations, sun-shading, and types of glazing) (Rahman et al., 2015, Nunes et al., 2013) [7,8], while there are other more recently devised techniques, such as ground and radiative cooling, which have been discussed by Brandl (2013) [9].

Nocturnal crossflow ventilative cooling involves using outdoor air during the night to remove heat or to store coolness in the building, considering that outside temperatures are lower than indoor temperatures. The aim of ventilative passive cooling is to lower the structure (thermally conditioned zone) temperature and postpone daytime temperature rises [10,11]. In the case of natural ventilation for office buildings, the preferable floor layout for such aeration is an open space with a large volume and with glazing on two opposite sides, so that cold air can enter, gather the warm air and flow out through the opposite side, as seen in Figure 3.

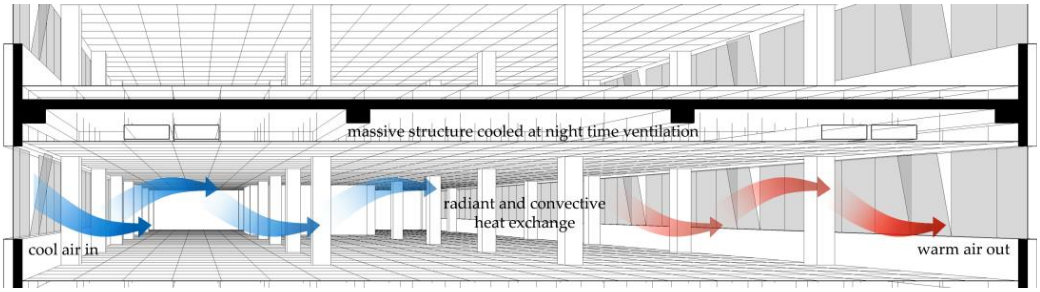

Figure 3. Nocturnal ventilative cooling scheme.

Several different approaches for passive solutions have been made with the goal of reducing cooling energy demand. Many studies have shown the possibilities of manipulating the solar irradiation that affects the building design characteristics. Freewan investigated the impact of external shading devices on office buildings (2014), as well as the impact of inclining of the building façades inward and outward on the south and north facades (2022) [12,13]. Wei et al. (2016) studied building forms such as window-to-wall proportions, number-to-floor forms and overall scales [14], while Premrov et al. (2018) investigated the optimal shape and proportions along with the appropriate orientation of buildings in warm climatic regions, finding that the building shape influences annual energy demand [15]. Caruso (2013) and Hemsath et al. (2015) studied building floor shapes as well as self-shading and solar-irradiance-protected buildings by developing non-rectangular, geometrically more complex floorplans, creating Building Energy Modelling (BEM) [16,17]. All of these studies focused on solar control and reducing the inlet of solar heat gains.

Breesch and Janssens (2005) made some measurements for night ventilation by single-sided and cross ventilation calculating parameters for thermal comfort, while Bayoumi (2018) studied natural ventilation conditions affecting healthy living and thermal comfort, focusing on optimal wind velocities, air exchange rates, and CO_2 concentration with the results indicating the potential for natural ventilation to be used to meet energy demand [18]. Furthermore, Oropa-Pérez (2019) studied the influence of integrated driving on the performance of different passive heating and cooling methods handling several features, such as mobility, maintenance, assembly, and consumables [19]. In addition, Samuel et al. (2013) discussed passive alternatives to mechanical ventilation for a healthy environment, energy, and cost savings [20]. Nevertheless, these studies were concerned with healthy living, thermal comfort, passive cooling advantages in general, etc. rather than with actual energy savings determined by nocturnal cooling loads.

Some researchers have carried out passive cooling calculations. Van der Maas, Roulet, and Flourentzou investigated several times (1991, 1993, 1996) a stacking effect and calculations for lowering temperatures inside buildings considering the air that flows upward inside buildings. Nunes et al. (2013) studied earth-to-air technology [8], while Breesch et al. (2004) calculated the passive cooling of buildings through both day ground cooling and the night ventilation method. In their research, night ventilation was driven by wind and thermally (stack) generated pressures [21]. Kaduchová et al. (2021) searched for a numerical simulation of passive cooling beams and optimisation of the design parameters of ceiling passive cooling convectors to increase the cooling capacity [22]. After all, their results and conclusions were directed toward improving the physical characteristics of buildings, such as façade insulation and shading [23–28].

Pesic et al. (2018) analysed eight reference geolocations on the southern European Mediterranean coast, including Split. Their focus was on the availability of climate potential for natural ventilation for each city corresponding to human hygrothermal conditions. The second part of the study referred to possible cooling energy savings obtained by the stack-pressure effect ventilation strategy. In Split, the next day cooling demands on annual levels were found to be reduced by 25% by using night natural ventilation only and 28% by using both day and night ventilation, supplemented by air conditioning during the day [29].

This paper proposes a methodology to determine the effects of cross ventilation and passive cooling on the energy states of buildings. Moreover, a method to determine the passive ventilation heat loss coefficient is given for a model building example. The focus is on disposing of the heat absorbed and embedded in the construction from the previous day, as a method to reduce cooling energy demand, rather than to prevent solar heat gains. Finally, the savings in annual energy consumption for crossflow cooling were calculated, whereupon cases with and without passive cooling were compared. Night ventilation influencing factors such as climate conditions and building's physical and aerodynamic characteristics were considered as the main inputs for the methodology and calculations.

According to Zamani et al. (2018) and Datta (2001), under climate conditions, there are the following factors: the outside temperature, diurnal temperature swing, wind velocity and direction, and relative humidity, while the most important physical characteristics of the building are the floor layout (preferable open spaces in large volumes), room sizes and orientations, window sizes and orientations, window shadings, envelope colour, and roughness, and landscape design [30,31].

The methodology was based on Computational Fluid Dynamics (CFD) analysis of the building and the dynamic (hourly) method of calculation. Visual Basic 2017 © programming language was used to create a mathematical simulation of heat loss due to passive ventilation. A method to obtain a passive cooling ventilation heat loss coefficient is described as well as its implementation using the calculation according to ISO 52016-1:2017 [32].

2. Methodology

This paper includes four sub-goals to determine the cooling potential of night ventilation.

(1) A model with physical characteristics was created: a prototype of the office building, which corresponds to the standard requirements and regulation conditions for the analysed areas. Moreover, defining building physical characteristics also requires determining heat accumulation, the heat loss coefficient by transmission and ventilation as well as internal and solar heat gains.
(2) The influence of climate conditions on passive cooling was investigated through model aerodynamic properties, such as the orientation of the openings, wind pressure onto the envelope, and the number of air exchanges.
(3) Four cases were defined: two cases for each climate zone, with and without passive night cooling.
(4) Measurements and simulations of passive cooling were conducted by the calculation of cooling energy demands along with the heat absorption of passively ventilated air.

2.1. Model Physical Characteristics

2.1.1. Heat Accumulation

The model used in the analysis is a six-story office building with a reinforced concrete skeleton construction, as shown in Figure 4, where the longer sides of the building are oriented toward the north and south. A rectangular pattern of 8 m × 8 m was used in the floor plan with overall footprint dimensions of 72 m × 24 m. The interfloors are massive concrete slabs supported by beams and columns, while the horizontal stability is ensured by two concrete cores.

The entire mass of the construction cannot be considered for heat accumulation because it is not fully exposed to internal air. In office buildings, the floors are often raised computer floors with massive gypsum boards and acoustic proofing in the floor interspace. Perforated gypsum board ceilings with acoustic fleece are implemented to improve internal air, and therefore the heat accumulation of the slabs and beams is neglected in the heat capacity calculation. For the calculation of the heat capacity of materials exposed to internal air, a maximum effective thickness of 0.1 m is accounted for. Therefore, the thermal effusivity of materials inside the zone is neglected. Table 1 shows the thermal mass included in the heat accumulation calculation, calculated using Equation (1):

$$C = m \times c \qquad [\mathrm{J/K}] \tag{1}$$

where C [J/K] is heat capacity, m [kg] is mass and c [J/(kgK)] is specific heat capacity.

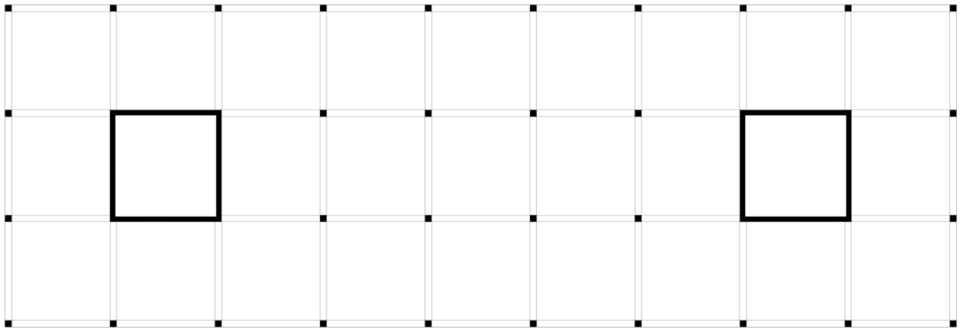

Figure 4. Analysed model load-bearing construction is a reinforced concrete skeleton.

Table 1. Constructions accounted for in the heat accumulation of the building.

Construction	Mass * m [kg]	Specific Heat Capacity c [J/kgK]	Heat Capacity C [MJ/K]
Gypsum linings	606,300	900	545.7
Partition walls	47,100	900	42.4
Concrete columns	273,600	1000	273.6
Concrete parapet	240,000	1000	240
Core walls	921,600	1000	921.6
Total			2023.3

* Mass of elements exposed to internal air, with maximum effective thickness of 0.1 m.

2.1.2. Transmission and Ventilation Heat Loss

The transparent envelope of the façade consists of double-glazed insulated glass units (IGU) inside the aluminium frames with a thermal break above a parapet wall. Figure 5 shows the shape of the building and the disposition of the fixed and top-hung window openings. Façade panes in the model are 100 × 200 cm, where every sixth window is specified as a top-hung opening, while the rest are fixed windows.

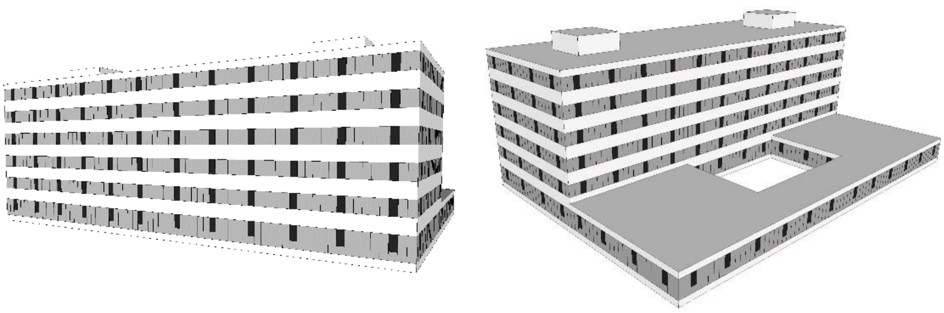

(**a**) (**b**)

Figure 5. Scheme of a model used in the analysis: (white) walls, (dark grey) fixed glazing, (black) top hung windows; (**a**) south façade, (**b**) north façade.

In Table 2, the main window characteristics are shown, which are later used in calculations. Double glazing is implemented instead of triple glazing since the internal and solar heat gains significantly reduce heating loads during winter. The heat transfer coefficient of the selected glazing U_{gl} [W/(m^2 K)] is 1.10 [33]. The frame factor, F_{fr} [−], is the ratio of the glazing area and the entire window area, influencing not only solar heat gains but also the U [W/(m^2 K)] value. The difference in the frame factor between fixed and casement window is visible in Figure 6.

Table 2. Window characteristics.

Type	Fixed	Top Hung
Unit size		
Width [mm]	1000	1000
Height [mm]	2000	2000
Glazing		
A_{gl} [m^2]	1.82	1.29
U_{gl} [W/(m^2 K)]	1.10	1.10
Frame		
A_{fr} [m^2]	0.18	0.71
U_{fr} [W/(m^2 K)]	1.80	1.80
Spacer		
l [m]	5.76	4.96
Ψ [W/mK]	0.04	0.04
F_{fr} [−]	0.91	0.64
U_w [W/(m^2 K)]	1.28	1.45

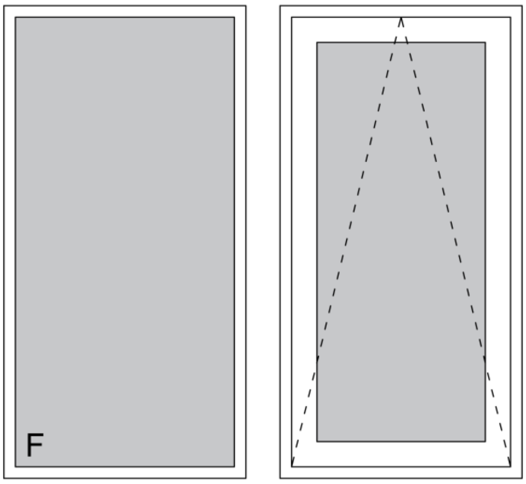

Figure 6. Characteristics of the façade used in the analysed model.

In Zagreb (continental climate), the parapet walls and interfloor construction above the underground garage are thermally insulated with 15 cm mineral wool, and the roof is insulated with 20 cm mineral wool, while in Split (maritime climate), there is 10 cm of mineral wool in the parapet walls and interfloor construction above the underground garage, and 15 cm on the roof. According to the Technical Regulation on the Rational Utilization of Energy and Thermal Insulation of Buildings (Official Gazette 102/2020) [34], these are typical thermal insulation thicknesses for new nearly zero energy buildings (nZEB) for these geographical regions [1,34].

The total heat loss coefficient by transmission between the building and the environment is 5964.5 W/K for the building in Zagreb and 6681.3 W/K for the building in Split (Table 3).

The ventilation heat loss coefficient (H_{ve}) was calculated using Equation (2):

$$H_{ve} = \frac{V_{air} \times \rho_{air} \times c_{air} \times n}{3600} \qquad [\mathrm{W/K}] \tag{2}$$

where H_{ve} [W/K] is the ventilation heat loss coefficient, V_{air} [m^3] is the volume of air, ρ_{air} [kg/m^3] is the air density, c_{air} [J/kgK] is the specific air heat capacity and n [h^{-1}] is the number of air exchanges per hour.

Table 3. Total heat loss coefficient by transmission between the building and the environment.

Building Element	Thermal Insulation/ Thickness Zagreb/Split [cm] Heat Conductivity c [W/mK]	Area A [m^2]	Zagreb		Split	
			Heat Transfer Coefficient U [W/(m^2 K)]	Heat Loss Coefficient $Htr = A * U$ [W/K]	Heat Transfer Coefficient U [W/(m^2 K)]	Heat Loss Coefficient $Htr = A * U$ [W/K]
Fixed glazing	Aluminium frame with double glazing	2400	1.28	3072	1.28	3072
Window opening	Aluminium frame with double glazing	480	1.45	696	1.45	696
Parapet wall	Mineral wool 15/10 cm (λ = 0.035) W/mK)	2560	0.22 *	691.2	0.32 *	947.2
Roof	Mineral wool 20/15 cm (λ = 0.035) W/mK)	3072	0.17 *	675.8	0.22 *	829.4
Intermediate floor above garage	Mineral wool 15 /10 cm (λ = 0.035) W/mK)	3072	0.22 *	829.4	0.32 *	1136.6
Total heat loss coefficient by transmission, *Htr* [W/K]				5964.5		6681.3

* The influence of thermal bridges is approximated with additional ΔU_{TM} = +0.05 W/(m^2 K).

The mechanical ventilation heat loss coefficient with the heat recovery module was determined by Equation (3):

$$H_{ve,mech,hru} = (1 - \eta_{hru}) \times H_{ve} \qquad [\mathrm{W/K}] \tag{3}$$

where $H_{ve,mech,hru}$ [W/K] is a heat loss coefficient by mechanical ventilation with a heat recovery unit, η_{hru} [−]) is the heat recovery unit efficiency, and H_{ve} [W/K] is the ventilation heat loss coefficient. In the model, a 75% efficient crossflow plate heat exchanger is implemented in Zagreb. The heat loss coefficient of the mechanical ventilation system, $H_{ve,mech,hru}$ for the continental climate is 3656 W/K.

In the maritime climate, temperatures are warm enough to avoid the need for heat exchange during the winter. The heat loss coefficient of the mechanical ventilation system without heat recovery, $H_{ve,mech}$, is calculated by Equation (2) and totals 14,623 W/K for Split.

2.1.3. Internal and Solar Heat Gains

The analysed internal heat gains included heat dissipation from people, computer equipment, lighting, and HVAC auxiliary energy, which are all included in Table 4 [35].

Table 4. Power consumption and heat gains from users, equipment, lighting, and HVAC systems.

People Equipment	Mean Value Power	Units	Density
People *	110	W	1/12 m^2
Desktop *	53.3	W	1/1 person
Monitor *	32	W	1/1 person
Printer *	495	W	1/10 persons
Multi-function *	1301.8	W	1/50 persons
Lighting	77,882	W	1/4 m^2
Ventilation	27,500	W	–
AC auxiliary power	8000	W	–
Total people	6.42	W/m^2	
Total equipment	9.38	W/m^2	
Total lighting	1.75	W/m^2	
Total ventilation	2.5	W/m^2	
Total AC auxiliary power **	0–0.72	W/m^2	
Overall	20.05	W/m^2	

* People and office equipment were calculated with the simultaneity factor 0.7, ** Auxiliary power is proportional to the cooling load.

The number of occupants in open space office buildings reaches up to one user per 12 m^2 of floor area. The heat generated by a person depends on their activity. Light work at a computer desk will generate approximately 110 W of heat [36,37].

The number of desktop computers with monitors was estimated to be one computer per person, while the number of printers was one printer for ten people. A contemporary computer generates 53.3 W, a monitor generates 32 W, and a printer generates up to 495 W of heat. During the night, it was assumed all the computers were on standby mode, with a heat generation of 10 W per computer assumed. A simultaneity factor of 0.7 was accounted for; it is assumed that a full capacity of workers is at their desks 70% of the time from 7:00 am to 8:00 pm [38].

The total required power for installed lamps depends on the needed light level intensity, the light emission, and the height of the lamps from the working surface. Even with LED lighting, installed power can exceed 7 W/m^2. However, artificial lighting is not used in the entire building and not constantly, especially during the summer (cooling period) when the amount of natural light is sufficient most of the day. In the analysed model, the average power of lighting was estimated to be 7 W/m^2, and only one-quarter of the building area is lit during the occupied period in summer [38].

Most of the auxiliary power used for ventilation and air circulation remains in the building as dissipated heat. The volume of air in the analysed building is 33,379 m^3, and the required volumetric flow is 43,392 m^3/h. For such an amount of airflow, a total fan power of 53.0 kW was estimated (26.5 kW inlet and 26.5 kW outlet fan). Heat dissipated from an inlet fan during ventilation worktime was included in the heat gain analysis.

Selected cooling units inside the workspace area are parapet and ceiling fan coils. Total ventilator power inside the fan coil units was estimated to be 10 W per 1000 W of cooling power. The maximum cooling load in the model building for Zagreb is 635 kW and 564 kW for Split, meaning that for the maximum auxiliary power cooling load in Zagreb, an additional 6.4 kW of heat will be added to the conditioned zone, and 5.6 kW in the case of Split. Total lighting, ventilation, and AC auxiliary power are expressed regarding the useful floor area in Table 4.

Solar irradiation on glazed surfaces was calculated according to (EN) ISO 52010-1:2017 (Energy performance of buildings—External climatic conditions—Part 1: Conversion of climatic data for energy calculations), which includes data connected to location, orientation, tilt angle, solar irradiance, etc [39]. The meteorological dataset was obtained from PVGIS [(c)] [5]. The most effective sun protection would be outer sun shading. However, it can be an inappropriate choice for tall buildings due to strong winds. Instead, the less effective solution was used, the glass with a low solar factor in combination with internal sunshades. The solar factor of the chosen glazing, g $[-]$, is 0.35 and the sunshade coefficient, F_{sh} $[-]$, of the inner shades is 0.9 (dark colour or high transparency) according to Technical Regulation on the Rational Utilization of Energy and Thermal Insulation of Buildings (Official Gazette 102/2020) [34].

Figure 7a,b shows the heat gains for the office building in Zagreb on 6 August and in Split 13 July, respectively. On these days, cooling loads had the highest values. Internal heat gains include people, office equipment, lighting, and auxiliary power for ventilation and air conditioning. In the model, maximum solar heat gains surpassed all other heat gains combined, due to the choice of solar control: glazing of a low solar factor, without outer sunshades. On 6 August, in Zagreb, total solar heat gains were 308 kW, and on 13 July in Split, they were 218 kW. Peak solar gains during the year were 356 kW for the building in Zagreb and 386 kW for the building in Split.

A summary of collected data from the physical building characteristics of the research is shown in Table 5.

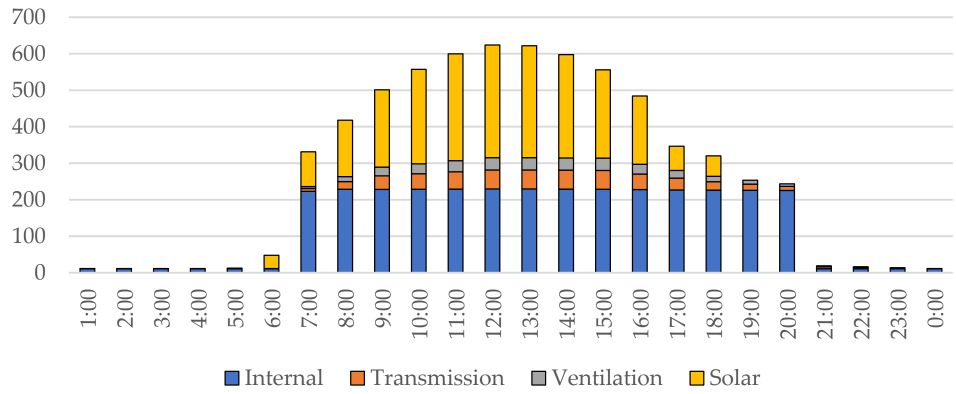

(**a**)

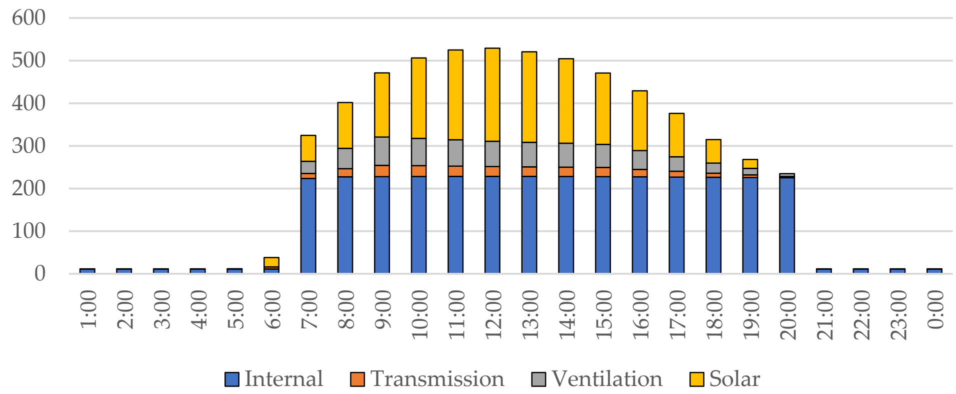

(**b**)

Figure 7. Total heat gains (kW) for 6 August in Zagreb (**a**) and 13 July in Split (**b**).

Table 5. Initial physical characteristics of the building.

Building Information	Symbol	Continental Climate Zagreb	Maritime Climate Split
Cooling temperature	$\theta_{int,set,C}$ [°C]	26	26
Useful area	$A_{k,use}$ [m^2]	11,126.4	11,126.4
Air volume	V_{air} [m^3]	33,379.2	33,379.2
Heat accumulation	C [MJ/K]	2023	2023
Heat loss by transmission,	H_{tr} [W/K]	5964.5	6681.3
Internal heat gains occupied	$q_{int,occ}$ [W/m^2]	20.05	20.05
Internal heat gains auxiliary	$q_{int,aux}$ [W/m^2]	0–0.57	0–0.51
Internal heat gains not occupied	$q_{int,noc}$ [W/m^2]	1	1
Air exchanges per floor area	V_A [m^3/(hm^2)]	4	4
Heat recovery unit efficiency	η_{hru} [−]	0.75	0
Ventilation heat loss	$H_{ve,mech}$ [W/K]	3656	14,623
Air infiltration	n_{50} [h^{-1}]	1.5	1.5

2.2. *Influence of Climate Conditions on Passive Cooling*

2.2.1. Orientation of the Openings

The average annual windspeed, regardless of the direction, for Zagreb was 2.47 m/s and for Split was 3.77 m/s. The wind direction component parallel with the façade openings was neglected, while in the model, only the absolute component of the wind perpendicular to the façade is accounted for, as shown in Equation (4).

$$v_n = \left| v_{wind} \times \cos\left(\gamma_{fac} + \gamma_{wind}\right) \right| \qquad [\mathrm{m/s}] \tag{4}$$

where v_n [m/s] is the windspeed component normal to the façade surface, v_{wind} [m/s] is the windspeed measured at the height of 10 m, γ_{fac} [°] is the façade azimuth and γ_{wind} [°] is the wind azimuth.

2.2.2. Windspeed

In the meteorological stations, wind speeds are measured at the height of 10 m above the ground, according to EN 1991-1-4:2012/NA:2012 [40]. An air mass moving near the ground is slowed down by terrain roughness, which depends on the type of surface, resulting in different windspeeds depending on the altitude. The greatest terrain roughness is in urban areas, while the lowest is in open terrain and water, expressed by Hellman's coefficient, α [−]. Windspeed differences for different altitudes are expressed by the wind gradient, w [−] (Equation (5)). Figure 8 shows the wind gradients for urban areas and rural and flat terrain [41,42]. Since the windspeeds are different at different heights, different pressures are exerted on the envelopes of buildings, and a different number of air exchanges are expected on different floors.

$$w = \left(\frac{H}{10}\right)^{\alpha} \qquad [-] \tag{5}$$

Here, w [−] is the wind gradient, H [m] is the height from the ground and α [−] is Hellman's coefficient.

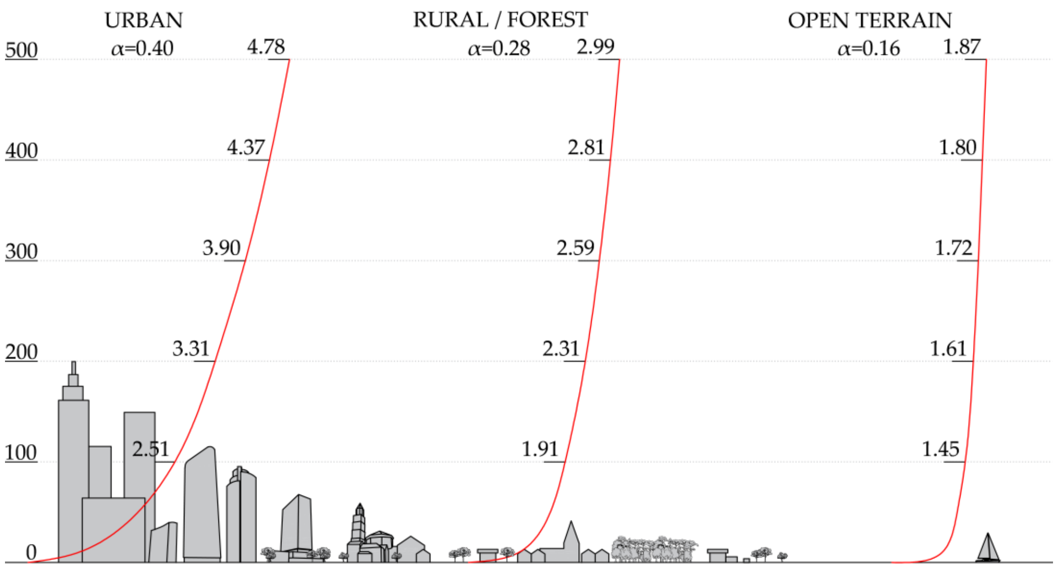

Figure 8. Wind gradients at different altitudes regarding terrain and windspeed measured on-site at a height of 10 m [43].

Top floors in high buildings are exposed to stronger winds than the wind at a height of 10 m, and lower buildings are exposed to slower winds. Average wind gradient calculation (Equation (6)) was used to determine the average windspeed affecting the building façade:

$$w_{avg} = \frac{\sum\left(A_{fl,fac} \times \left(H_{fl}/10\right)^{\alpha}\right)}{\sum A_{fl,fac}} \qquad [-] \tag{6}$$

where w_{avg} [−] is the average building wind gradient, $A_{fl,fac}$ [m^2] is the floor façade area, H_{fl} [m] is the floor height from the ground, and α [−] is Hellman's coefficient. The windspeed used in calculations of the number of air exchanges per hour is given in Equation (7):

$$v_{wind,avg,n} = w_{avg} \times v_n \qquad [\mathrm{m/s}] \tag{7}$$

where $v_{wind,avg,n}$ [m/s] is the average windspeed normal to the façade surface regarding the windspeed measured at 10 m, and v_n [m/s] is the windspeed component normal to the façade surface.

In the case of the north- and south-oriented façade, the average annual component of the wind perpendicular to the façade was 1.74 m/s in Zagreb and 2.63 m/s in Split. As seen in Figure 9, windspeeds at the top floor would be three times faster than those at the ground floor, and 40% faster than at the measured height of 10 m. In the urban area of terrain roughness, α = 0.40 (Figure 8), and the average wind gradient for the 24 m analysed model, w_{avg} was 0.98.

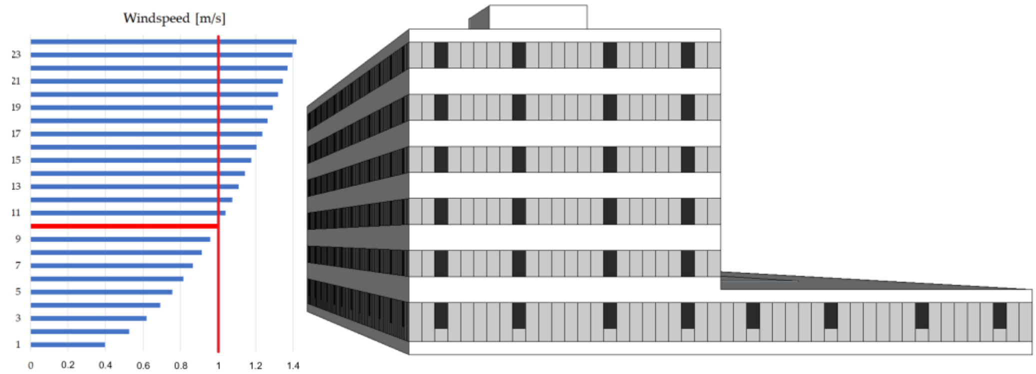

Figure 9. Wind gradient for 24 m tall building in urban area.

2.2.3. Wind Pressure on the Envelope

A CFD simulation was used to correlate windspeed with the number of air exchanges through the air pressure on the façade surface. The building model was created in 3d studio MAX 2016® and imported into the Simscale® simulation software, in which an incompressible fluid flow analysis was developed. The goal was to determine the pressure exerted on the façade on the windward (north) and leeward (south) sides of the building and to correlate them with windspeed.

The pressure differences at windspeeds of 1, 2.9, and 13 m/s were analysed, where 2.9 m/s was the average windspeed between Zagreb and Split, and the 13 m/s windspeed results for the average pressure of 50 Pa were found using CFD (Computational fluid dynamics) analysis. Figure 10 shows the pressure diagrams that were later used to determine the results regarding the pressure values in Table 6.

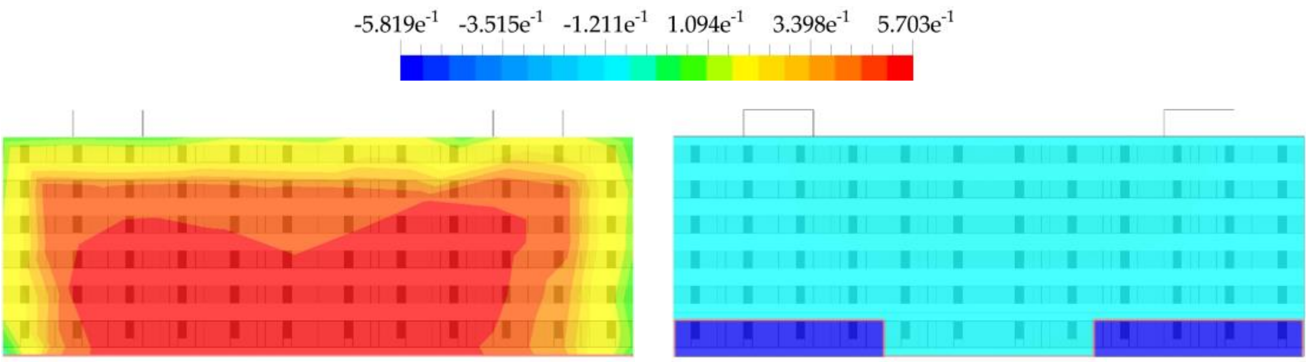

(**a**) (**b**)

Figure 10. Pressure differences on opposite sides of the building; (**a**) windward, north façade; (**b**) leeward, south façade, for the windspeed of 1 m/s.

Table 6. Pressure values on the facade and the air flow rate depending on the windspeed.

WINDSPEED, v_{wind} [m/s]	Pressure, p [Pa]				Volumetric Flow Rate, V_f [m^3/s]	Air Exchanges, n [h^{-1}]	n/v, F [s/(m.h)]
	Windward	Leeward	Difference	Average			
1	0.4	−0.2	0.6	0.3	1.47	3.06	3.06
2.9	3.7	−1.4	5.1	2.55	4.19	8.73	3.01
13	72	−30	102	51	18.7	38.96	3.00

2.2.4. Air Exchange Number

After the pressure differences on the opposite building sides were determined, only a 24 × 24 × 3 m layout segment was observed. There are four top-hung openings placed on both the north and south sides of the office area segment, making the total top-hung opening area on each side 3 m^2. The air exchange number obtained in the analysed segment was applied to the building model as a whole.

A more detailed model of the office workspace segment was created in Revit 2022® and imported into Simscale® for an incompressible fluid flow analysis, as seen in Figure 11. The goal of the second CFD analysis was to correlate the average air flow rate with the pressure differences on the windward and leeward sides.

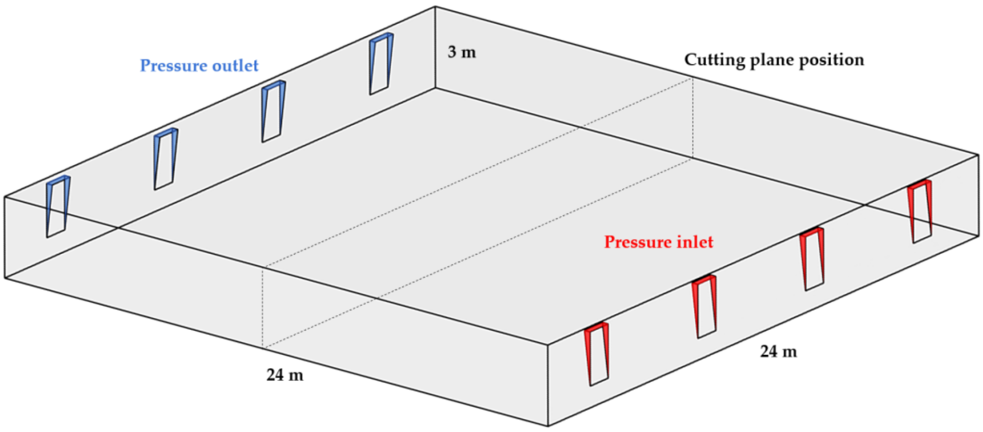

Figure 11. Disposition of pressure inlet and outlet openings.

Since cross ventilation is more effective [44] than single-sided ventilation, only cross-ventilation potential was analysed in this research.

Results of the CFD analysis regarding the number of air exchanges are also presented in Table 6. The results show a proportional relationship between the windspeed and the number of air exchanges. The formula (Equation (8)) used in the calculation is:

$$n_{ve,pass} = F \times v_{wind,avg,n} \qquad \left[\mathrm{h}^{-1}\right] \tag{8}$$

where $n_{ve,pass}$ [h^{-1}] is the number of air exchanges due to passive ventilation, F [s/(mh)] is the ratio factor between the number of air exchanges and windspeed, obtained from Table 6, and $v_{wind,avg,n}$ [m/s] is the average windspeed normal to the façade surface. For the analysed model, the chosen factor was rounded to 3.0. This factor, here acquired by CFD analysis, depends on the aerodynamic properties of the building, along with the number of openings and their disposition, which means this differs from building to building. Figure 12. shows the CFD airflow simulation through the observed layout segment in both section and floorplan.

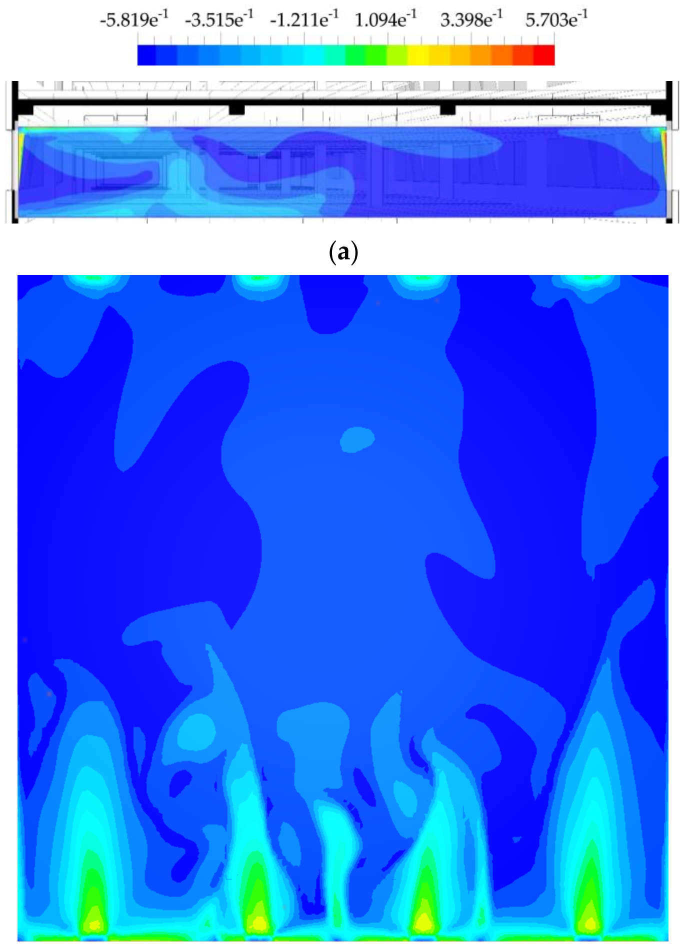

(a)

(b)

Figure 12. CFD airflow simulation; (**a**) section, (**b**) floorplan.

2.3. Passive Cooling Calculation

2.3.1. Cooling Energy Demand

During building use, all the fresh air that enters a building by natural or mechanical ventilation must be heated or cooled to the desired temperature. In that case, energy demand (Equation (9)) for heating or cooling the air for a period of time depends on the temperature difference and heat loss coefficient by ventilation.

$$Q_{air,H,C,nd} = (\theta_{set,\text{int},H,C} - \theta_e) \times H_{ve} \times t \qquad [\text{J}] \tag{9}$$

Here, $Q_{air,H,C,nd}$ [J] is energy for heating or cooling the air to the desired temperature, $\theta_{set,int,H,C}$ [°C] is the internal heating or cooling temperature, θ_e [°C] is the external air temperature, H_{ve} [W/K, W/°C] is the heat loss coefficient (for any kind of ventilation), and t [s] is the observing duration time.

2.3.2. Heat Absorption of Passively Ventilated Air

When a building is ventilated passively during the night, air that enters the building is passively heated or cooled only by internal surfaces in contact with the air. Air is ventilated through a building at a rate that is dependent on the number of air exchanges per hour. This means the heat is transferred from internal surfaces to the air only for a certain period. The faster the air moves through a building the less heat it absorbs, but a greater number of air exchanges are achieved.

Heat transfer between the surfaces and the air was calculated by a convective heat transfer coefficient. It can be expressed as a combination of natural and forced convection.

Forced convection includes heat transfer by a fluid in motion, while natural convection is caused by differences in the density of a fluid. Table 7 shows the average air velocity inside the building, taken from the Simscale® program (Figure 13), depending on the number of air exchanges per hour.

Table 7. Average air movement, $v_{air,int,avg}$ [m/s] inside office space regarding the air exchange number.

Air Exchanges Per Hour, n **[h^{-1}]**	**Average Air Velocity inside the Building,** $v_{air,int,avg}$ **[m/s]**
3	0.037
6	0.077
9	0.107

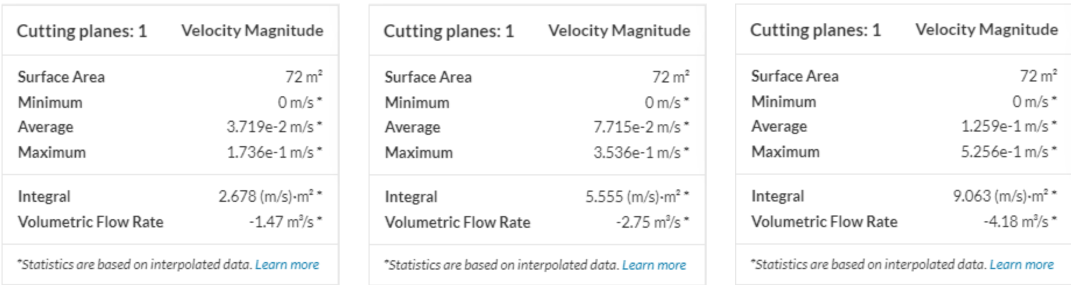

(**a**) (**b**) (**c**)

Figure 13. Average air velocity inside the building derived from (**a**) three, (**b**) six and (**c**) nine air exchanges per hour in the Simscale® program.

The conventional convective heat transfer coefficients used in calculations according to ISO 52016-1:2017 [32], corresponding to the building element orientation, are defined in ISO 13789:2017 [45]. They are presented as a constant and their values are 5.00 W/(m^2 K) for the floors, 2.50 W/(m^2 K) for the walls, and 0.70 W/(m^2 K) for the ceilings. When the calculation of convective heat transfer was performed, a substantial difference occurred in the case of smaller temperature differences, including the temperature difference between the surface and air.

Since the average movement of air inside buildings is insignificantly slow, in this model, only natural convection heat transfer component was accounted for. Figure 14 shows the convective heat transfer coefficient between the air and different surfaces inside the building at various temperature differences.

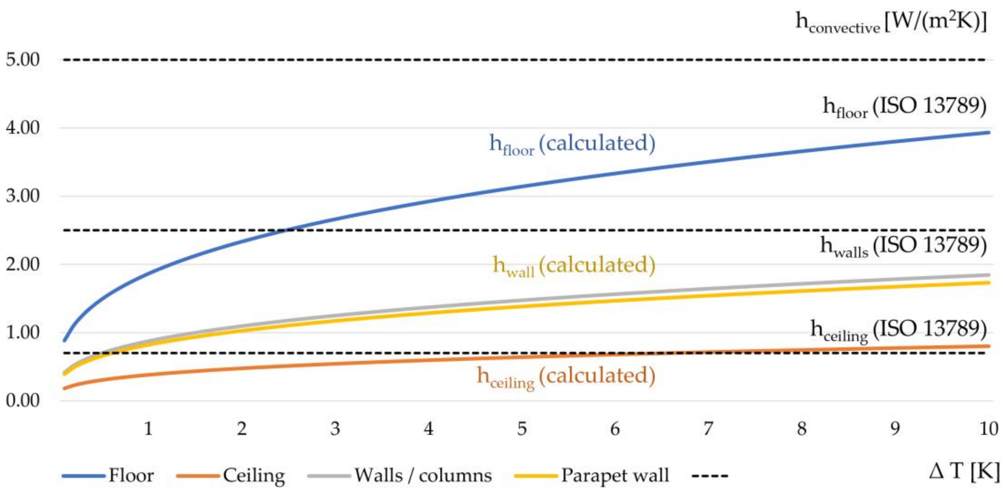

Figure 14. Convective heat transfer coefficient, h [W/(m^2 K)], for various surface inclinations and surface and fluid temperature differences, ΔT [K].

Heat transfer from surface to fluid (air) was calculated by Equation (10):

$$\phi_c = h \times A \times (T_w - T_\infty) = h \times A \times (T_{ztc} - T_{air,\text{int}}) \qquad [\text{W}] \tag{10}$$

where ϕ_c [W] is the heat flow rate by convection, h [W/(m^2 K), W/(m^2 °C)] is the surface coefficient of heat transfer, A [m^2] is the contact surface between the internal air and building element, T_w [K] is the surface (wall) temperature equal to T_{ztc} [K], which is a thermally conditioned zone temperature and T_∞ [K] is the ambient (fluid) temperature equal to $T_{air,int}$ [K], which is the internal air temperature.

The convective heat transfer coefficient, h [W/(m^2 K)], was determined by dimensionless numbers (Grashoff, Nusselt, Prandtl, Rayleigh, Reynolds, and Richardson numbers), which depend on the surface and fluid temperature, inclination, surface area, and fluid speed. Due to slow average air movement inside the building, heat transfer is dominated by natural convection [46]. The average convective heat transfer coefficient, h_{avg} [W/(m^2 K)], includes all internal surfaces and their convective heat transfer coefficients, and is calculated by Equation (11):

$$h_{avg} = \frac{\sum(h \times A)}{\sum A} \qquad \left[\text{W}/\left(\text{m}^2\,\text{K}\right), \text{W}/\left(\text{m}^2\,°\text{C}\right)\right] \tag{11}$$

where h_{avg} [W/(m^2 K), W/(m^2 °C)] is the average surface coefficient of heat transfer, h [W/(m^2 K), W/(m^2 °C)] is the surface coefficient of the heat transfer of the building element (floor, ceiling, wall/columns, parapet wall) and A [m^2] is a contact surface between the internal air and building element. The increase in air temperature was evaluated by the iterative calculation of Equation (12):

$$dT = \frac{(T_{ztc} - T_{air,\text{int}}) \times h_{avg} \times A \times dt}{m_{air} \times c_{air}} \qquad [\text{K}] \tag{12}$$

where dT [K] is temperature increase, m_{air} [kg] is the mass of the observed air, c_{air} [J/kgK] is the specific air heat capacity and dt [s] is duration time. Figure 15 shows the increase in air temperature inside the building due to heat transfer from internal surfaces regarding the time in which the air is in contact with the inner surfaces. The number of air exchanges per hour, n [h^{-1}], was added as a comparison to the time required for the quantity of air to pass through the building.

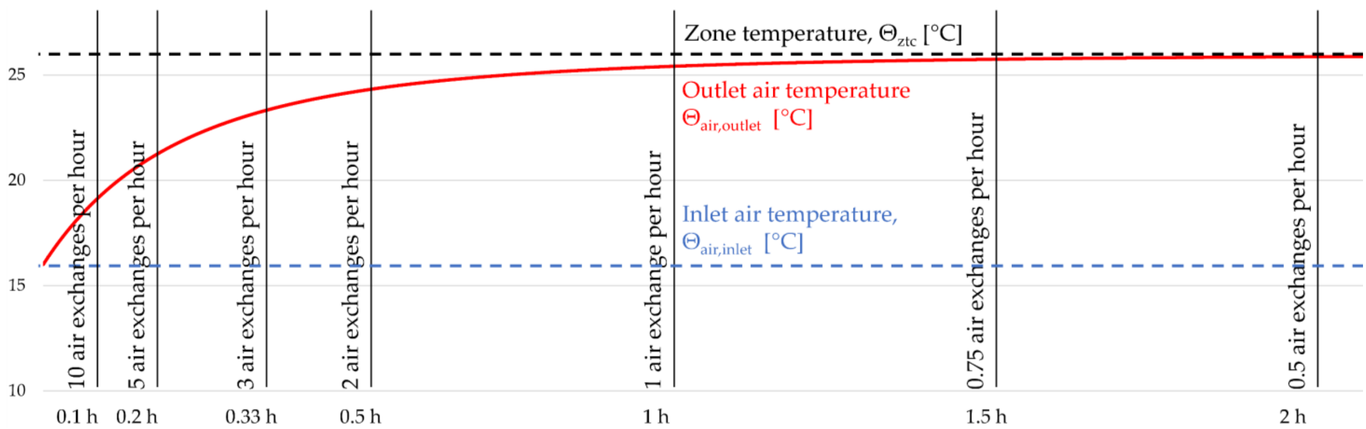

Figure 15. Outlet air temperature [°C] related to contact duration with inner surfaces for initial temperature difference of 10 °C.

Temperature differences between inlet and outlet air were calculated for every hour when passive cooling was in use. The ratio between the amount of absorbed heat and the maximum possible amount of absorbed heat was used to determine the heat loss coefficient by passive ventilation, $H_{ve,pass}$ [W/K], shown in Equation (13) and Figure 16. Since the amount of heat absorbed in the air is proportional to the temperature, the ratio can be obtained from the temperature differences between inlet and outlet air. The maximum temperature of the outlet air cannot exceed the temperature of the surfaces inside the building and the thermally conditioned zone temperature.

$$H_{ve,pass} = H_{ve} \times \frac{T_{air,outlet} - T_{air,inlet}}{T_{ztc} - T_{air,inlet}} \qquad [\mathrm{W/K}] \tag{13}$$

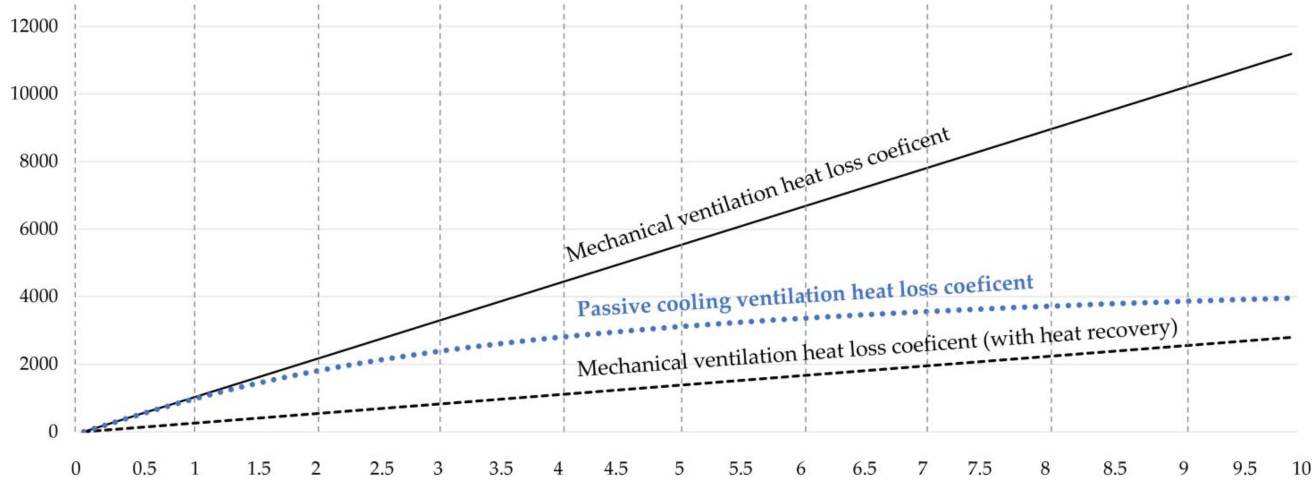

Figure 16. Heat loss coefficient by ventilation, H_{ve} [KW/K], depending on the number of air exchanges per hour, n [h^{-1}].

Here, $T_{air,outlet}$ [K] is the temperature of the air leaving the building, $T_{air,inlet}$ [K] is the temperature of the air entering the building and T_{ztc} [K] is a thermally conditioned zone temperature.

2.3.3. Mathematical Model

A mathematical model used to determine the cooling energy demand was developed using the Visual Basic 2017 © programming language. An iterative calculation of energy flow between the building and the environment was made according to ISO 52016-1:2017 [32]. A subroutine that determines the heat loss coefficient by passive ventilation was implemented in the calculation. The energy balance of a thermally conditioned zone during the occupied period was determined by Equation (14) and that during passive ventilation was determined by Equation (15):

$$Q_{ztc,t} = \left[\left(\frac{Q_{ztc,t-1}}{C_{ztc}} - T_e\right) \times (H_{ve} + H_{tr}) + \phi_{gn,\mathrm{int}} + \phi_{gn,sol}\right] \times \Delta t \qquad [\mathrm{J}] \tag{14}$$

$$Q_{ztc,t} = \left[\left(\frac{Q_{ztc,t-1}}{C_{ztc}} - T_e\right) \times \left(H_{ve,pass} + H_{tr}\right) + \phi_{gn,\mathrm{int}} + \phi_{gn,sol}\right] \times \Delta t \qquad [\mathrm{J}] \tag{15}$$

where $Q_{ztc,t}$ [J] is the energy state of the zone at the observed time, $Q_{ztc,t-1}$ [kWh] is the energy state of the thermally conditioned zone at the previous time interval, C_{ztc} [J/K] is the heat capacity of the thermally conditioned zone, T_e [K] is the outer air temperature, H_{ve} [W/K] is the heat loss coefficient by ventilation (natural or mechanical), $H_{ve,pass}$ [W/K] is the heat loss coefficient by passive ventilation, H_{tr} [W/K] is the heat loss coefficient by transmission, $\phi_{gn,int}$ [W] are the internal heat gains, $\phi_{gn,sol}$ [W] are the solar heat gains, and Δt [s] is the time interval.

2.4. Cases

For each referent city, regarding the climate zone, two cases according to the nocturnal ventilation type were created. A heat recovery system was included in Zagreb while winter conditions would not be satisfied. On the contrary, winters in Split are mild, and heat recovery is not required. The passive cooling calculation was performed as in the aforementioned *Methodology* section.

2.4.1. Continental Climate Case 1a

During the occupied period, the building is ventilated mechanically with the heat recovery system. During the night, ventilation is off, and windows are not opened. Air is exchanged only by unwanted infiltration.

2.4.2. Continental Climate Case 2a

During the occupied period, the building is ventilated mechanically with the heat recovery system. During the night, ventilation is off, and top-hung windows are opened. Air is exchanged by natural cross ventilation. If the inside temperature drops below 20 °C, the windows are closed by an automatic controller.

2.4.3. Maritime Climate Case 1b

During the occupied period, the building is ventilated mechanically (without the heat recovery system). During the night, ventilation is off, and windows are not opened. Air is exchanged only by unwanted infiltration.

2.4.4. Maritime Climate Case 2b

During the occupied period, the building is ventilated mechanically (without the heat recovery system). During the night, ventilation is off, and top-hung windows are opened. Air is exchanged by natural cross ventilation. If the inside temperature drops below 20 °C, the windows are closed by an automatic controller.

3. Results

In Table 8, results are shown as the annual specific cooling energy demand, $Q''_{C,nd}$ [kWh/(m^2 a)] for each case. Specific cooling energy demands show the total cooling energy needed in the building regarding the useful floor area.

Table 8. Results of annual cooling energy needs for all cases.

Specifics	Continental Climate		Maritime Climate	
	Case 1a	**Case 2a**	**Case 1b**	**Case 2b**
Heat recovery	Yes	Yes	–	–
Natural night ventilation	–	Yes	–	–
Specific cooling energy need, $Q''_{C,nd}$ [kWh/(m^2 a)]	66.41	37.48	53.38	36.18

3.1. Continental Climate

For the analysed model in the continental climate, Case 1a was a referent model where mechanical ventilation with a heat recovery unit was used during the occupied period, while during the night the mechanical ventilation was off. In Case 2a, mechanical ventilation with heat recovery was used during the day, but during the night, passive cooling was implemented. The specific cooling energy need $Q_{C,nd}$ [kWh/(m^2 a)] was calculated to be 738,885.5 kWh in Case 1a, and 417,054.5 kWh in Case 2a. The annual cooling energy need with passive cooling was found to be reduced by 43.5%.

Cooling energy needs, temperatures, and windspeeds are shown for five days in July in Figure 17. Among the chosen days, there were days when passive cooling had no effect and days when it had a substantial effect.

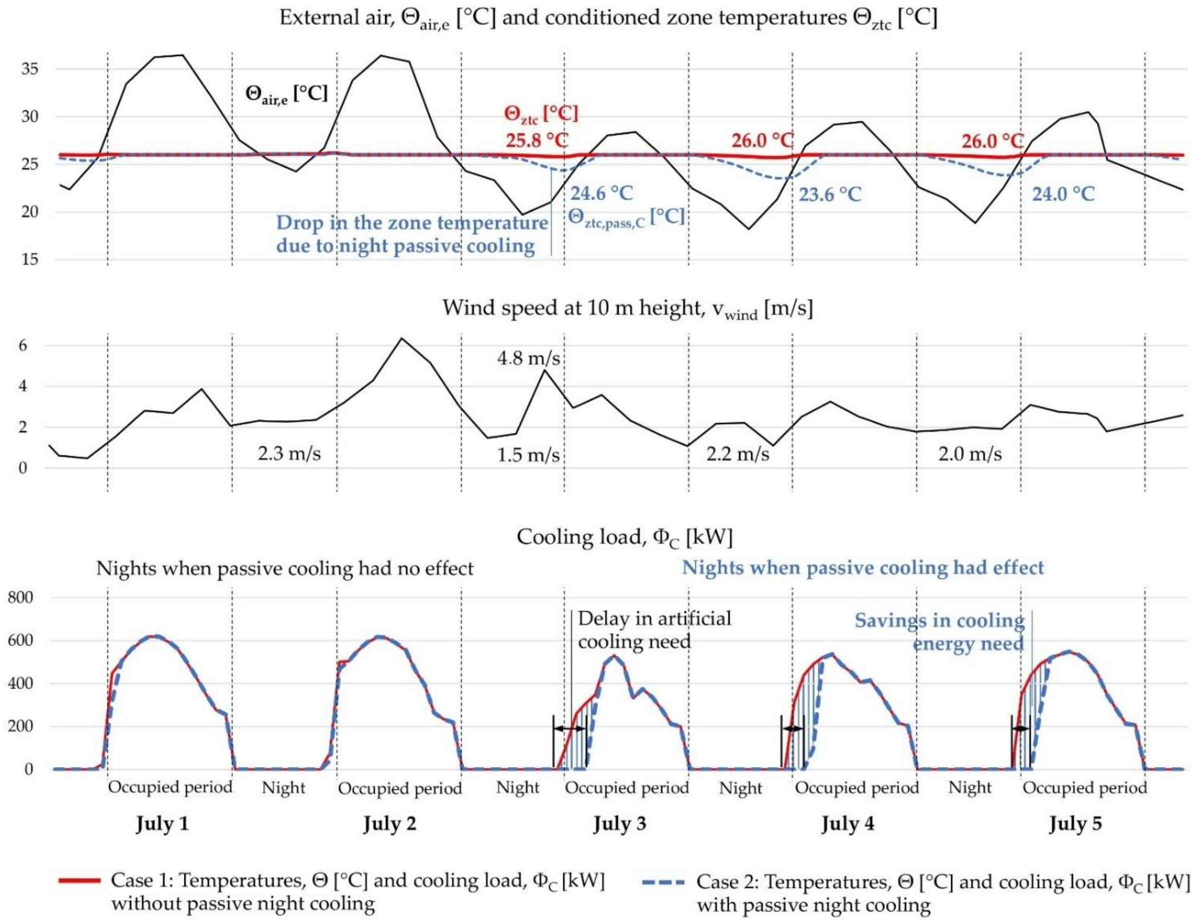

Figure 17. Results comparison for cases 1a and 2a in Zagreb.

In Case 1a, without the night ventilation, the heat stayed trapped inside the building and was lost only by transmission and unwanted air infiltration. This means minimal heat loss will take place since the envelopes of new buildings are both energy efficient and airtight. The temperature of the thermally conditioned zone (shown in the red line) did not drop during the night. The occupancy period on the next day began with the zone temperature at the upper limit of the inner set-point cooling temperature. Internal and solar heat gains accumulated in the building and caused the temperature to rise. As the temperature exceeded the set-point cooling temperature, artificial cooling was needed immediately at the start of the day.

Case 2a shows the results with night ventilation implemented. In this case, some of the heat can be ventilated by the air. The days with warm nights or no wind would not have had a significant effect on passive cooling (e.g., days 1 and 2 July), but colder, windy nights would have cooled down the building by several degrees, which is enough to delay the need to use air conditioning by several hours (e.g., days 3, 4 . . . July). Inner temperatures with passive night cooling (shown in the blue dotted line) dropped during the night only by several °C. At the start of the occupancy period on the next day, the zone temperature was approximately 2 °C lower than the interior set-point cooling temperature. Internal and solar heat gains again caused the temperature to rise in the building.

However, in this case, the initial temperature was not at the upper limit of the set-point cooling temperature. Heat was absorbed in the building and the temperature rose, but a few hours were needed to exceed the set-point cooling temperature. This way, artificial cooling is not needed immediately at the start of the day, but rather a few hours later. Although the drop in temperature is only by a few °C, the cooling need is delayed for hours. The savings regarding the cooling energy need are mostly because of those few hours at the start of the day when artificial cooling is not required.

3.2. Maritime Climate

For the analysed model in the maritime climate, Case 1b was a referent model where mechanical ventilation (without a heat recovery unit) was used during the occupied period, while during the night, the mechanical ventilation was off. The specific cooling energy need $Q_{C,nd}$ [kWh/(m^2 a)] calculated for Case 1b is 593,931.8 kWh. In Case 2b, mechanical ventilation was used during the day, but during the night passive cooling was implemented, with a specific cooling energy need of 402,581.5 kWh. Passive night cooling reduced the annual cooling energy need by 32.2% (Case 2b).

Building envelope and HVAC systems in continental climates have to be optimised for both winter and summer use. In the Mediterranean climate, envelope and HVAC systems can be focused primarily on the cooling period, which can result in less energy consumption for cooling despite the higher temperatures and solar radiation. Compared to the continental climate, the potential for savings is somewhat lower due to higher night temperatures, but still considerable.

The cooling energy need, temperatures, and windspeeds are shown for five days in July in Figure 18. Without the passive ventilation, the drop in inner temperature (shown in the red line) during the night was small, up to 0.5 °C. As seen for Case 1a (continental climate), the use of the building on the next day will quickly cause the temperature to exceed the inner set cooling temperature and artificial cooling will be required at the start of the day.

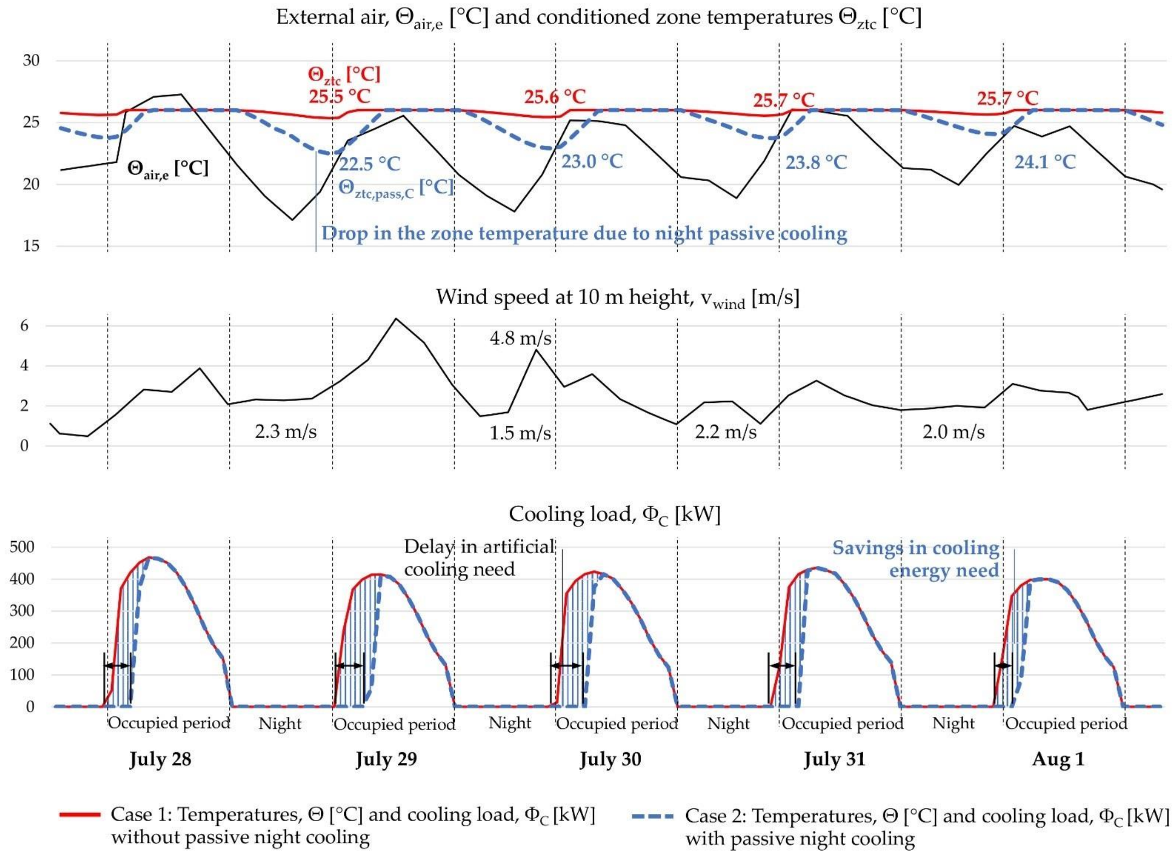

Figure 18. Results comparison for cases 1b and 2b in Split.

When night passive cooling was implemented (Case 2b), a greater drop in temperature can be observed. During the night, the inner temperature dropped approximately 2 °C more compared to the case without passive night cooling. As seen for Case 1b, at the start of the day, the internal temperature was lower than the set-point cooling temperature, and hours will pass before the temperature increases above this temperature. On the days shown for the maritime climate, the night temperatures dropped below 20 °C, so a delay in artificial air conditioning need was visible at the start of each day.

3.3. Annual Savings in Cooling Energy

Figure 19a,b shows savings in cooling energy need during the year for both climates. Annual savings are the sum of the daily savings described in the previous sections. At the start and at the end of the annual cooling period there were days when passive night cooling nullified the need for artificial cooling and therefore shortened the annual cooling period. The period for artificial cooling need was shortened by 21% for the continent and by 34% for the maritime climate. In both cases, a few days with negligible cooling energy need at the start and the end of the cooling season were neglected.

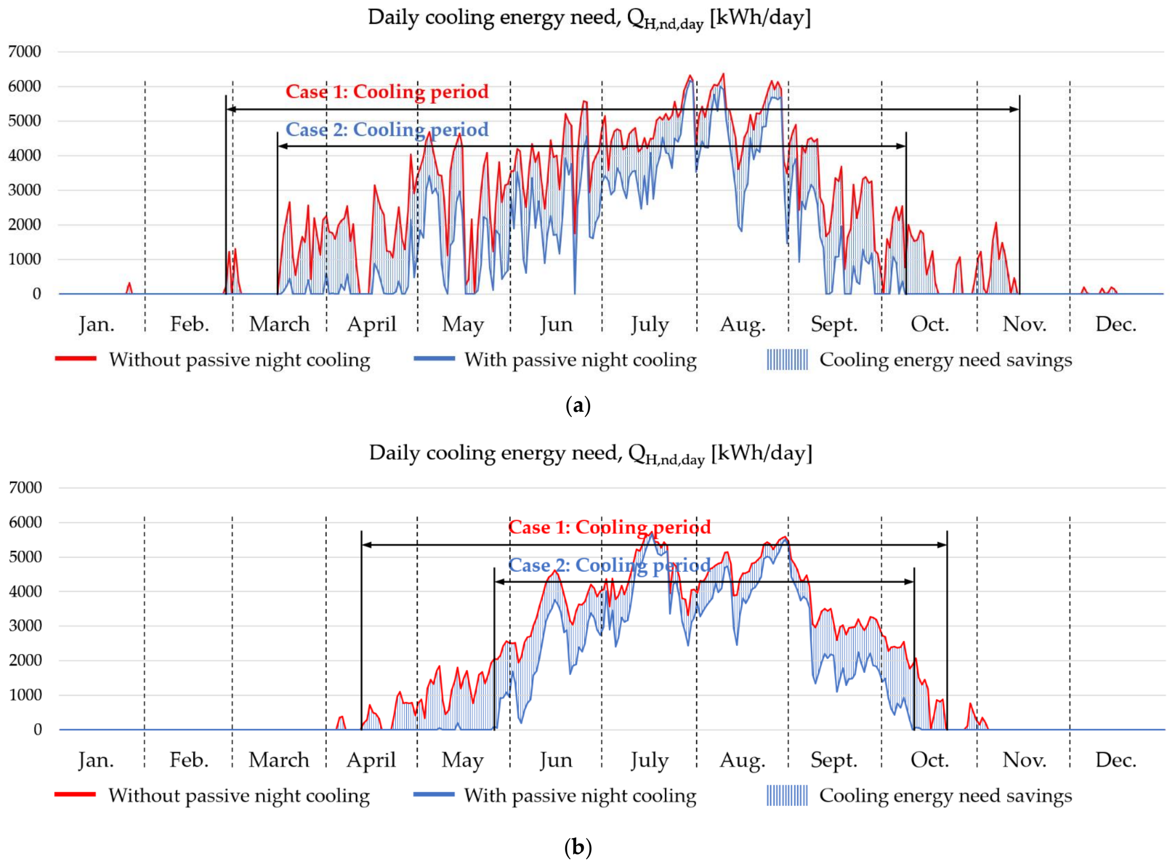

Figure 19. Annual cooling energy need with and without passive night cooling in (**a**) Zagreb and (**b**) Split.

4. Discussion

Although crossflow natural cooling is foreseen to be performed during the unoccupied period only, the conditioned zone temperature should drop enough to postpone the need for air conditioning during the next day. This delay in the need for artificial cooling presents the greatest savings in cooling energy demand. A daily delay in cooling needs takes place, and on an annual basis, the start of the cooling period is postponed, and the end of this period is shortened by a few weeks.

During the past few decades, several studies and calculations on this topic have been made. Attempting to achieve better thermal comfort, Van der Maas, Flourentzou, and Roulet conducted research on emphasising the diurnal temperature difference and lowering the following's day internal peak temperature, by investigating stack-driven ventilation. They noticed a significant drop in temperature during the unoccupied period, obtaining a ventilation rate of 10 air changes per hour from the initial 20 ± 0.5 °C to the new surface temperature of 18.8 °C and the air temperature of 15.9 °C [23–28]. Rahman (2015) used a solar chimney method that maintained 4–5 °C below the outside ambient temperature and about 2–3 °C below the reference room temperature (without solar chimney) for 21st May [7]. Pfafferoth made a contribution using ground cooling calculations that resulted in a drop of 0.9 °C in the inlet air temperature [10].

In this paper, a drop of 0.2 °C without crossflow ventilation, and from 1.4 to 2.0 °C with passive cooling was observed in the continental climate and up to 3 °C in the maritime climate. Although all the approaches used different types of passive cooling, this paper matched the results of all these approaches, that is, the thermally conditioned zone temperature differed for cca 1–2 °C before and after performing night passive cooling.

Nevertheless, the main point of this paper was to calculate annual energy savings. Pesic et al. (2018) found that stacking effect ventilation can reduce energy demand in a range from 22% to 28% in areas of Split, Athens, and Nicosia through day and night natural ventilation as the most effective cooling mode, comparing the results to other geolocations in the southern Mediterranean area with higher potential, such as Barcelona, Marseille, and Rome with 48% to 52% of reduction. In Split, together with Athens and Nicosia, the climate potential for natural ventilation is lower due to more unfavourable summer weather conditions, that is, higher overall temperatures [29].

In this study, savings of the annual cooling energy need with the cross ventilation passive cooling were calculated to be 43.5% for the continental climate, and 32.2% for the maritime climate, shortening the period with artificial cooling need by 21% in Zagreb and 34% in Split.

Besides this, it is important to say that this building model included only moderate solar control attributes (double glazing with a low solar factor of 0.35, and only inner sunshades). Raising the solar control performance of the building would lower heat gains and make the temperature difference even higher. Nevertheless, the outcome showed better-than-expected results in saving energy needs due to intensive passive cross ventilation. Not only can passive cooling contribute to improving thermal comfort, but it can also optimise the balance between costs and indoor air quality, as well as improve the environmental impact and CO_2 emissivity [47]. Finally, it is important to say that this calculation method is applicable to any location, climate, and physical characteristics.

5. Conclusions

The great potential of passive night cooling is shown in this research. The focus was on an office building with a substantial heat gain from users and equipment. An office building was selected because it is vacant during the night, which makes the use of passive night cooling ventilation easier. In the case of buildings with fixed glazing and an airtight and energy-efficient envelope, the heat stays trapped inside the building when ventilation is off during the night, but if natural ventilation is enabled through windows, some heat can be ventilated out naturally.

Different night cooling potential is shown in temperate continental and Mediterranean climates. A greater difference in day and night temperatures, as well as greater windspeeds during the night, will lead to greater night cooling effects. Summer day temperatures can be equally high for both the maritime and continental climates, but the diurnal temperature difference is greater in the continental climate. However, the possibility of cross ventilation will ensure a large number of air exchanges even at low ambient windspeeds and will significantly cool down the building.

Although night ventilation shows great potential for cooling energy savings, its use might not be applicable in every typology. In residential buildings, draft and traffic noise can discourage the use of night passive cooling by windows, and on ground floors, opened windows can present a security risk. Furthermore, there are buildings in which natural passive ventilation might not be possible at all. However, openings for passive cooling can be different types of hatches or valves in the envelope of a building, which can widen the use of passive cooling for more types of buildings or eliminate some of the disadvantages mentioned.

Author Contributions: Conceptualization, Z.V. and M.B.; methodology, Z.V., M.B. and M.N.M.; software, M.B.; validation, Z.V.; formal analysis, Z.V., M.B. and M.N.M.; investigation, M.B. and M.N.M.; resources, Z.V.; data curation, Z.V.; writing—original draft preparation, M.B. and M.N.M.; writing—review and editing, M.N.M.; visualization, M.N.M.; supervision, Z.V. and M.B.; project administration, Z.V.; funding acquisition, Z.V. All authors have read and agreed to the published version of the manuscript.

Funding: The research was conducted as part of the *Development of a double facade with hermetically sealed cavity H-CCF* project funded by the European Union from the European Regional Development Fund.

Conflicts of Interest: The authors declare no conflict of interest.

Nomenclature

List of Symbols		Units	Subscripts	
A	area	[m^2]	*air*	air
C	heat capacity	[J/K]	*A*	appliances
c	specific heat capacity	[J/K]	*an*	annual
F	factor	[−]	*avg*	average
g	glazing solar factor	[−]	*aux*	auxiliary
H	height	[m]	*C*	cooling
H	heat loss coefficient	[W/K, W/°C]	*c*	convection, convective
h	surface coefficient of heat transfer	[W/(m^2 K), W/(m^2 °C)]	*day*	daily
m	mass	[kg]	*e*	external, outdoor
n	number of air exchanges per hour	[1/h]	*el*	element
P	power	[W]	*fac*	façade
p	pressure	[Pa]	*f*	flow
Q	quantity of heat	[J, kWh]	*fl*	floor
q	heat flow density	[W/m^2]	*fr*	frame
qv	air volume flow rate	[m^3/h]	*gl*	glazing
T	thermodynamic temperature	[K]	*gn*	gain
t	time	[s]	*h*	hourly
U	heat transfer coefficient, thermal transmittance	[W/(m^2 K), W/(m^2 °C)]	*hru*	heat recovery unit
V	volume	[m^3]	*int*	internal, indoor
v	speed, velocity	[m/s]	*ld*	load
w	wind gradient	[−]	*m*	monthly
			mech	mechanical (ventilation)
Greek letters			*n*	normal
			nd	need
α	Hellman factor	[−]	*noc*	unoccupied period
γ	azimuth angle	[°]	*occ*	occupied period
η	efficiency	[−]	*oel*	opaque element
θ	Celsius temperature	[°C]	*pass*	passive
ρ	density	[kg/m^3]	*set*	set-point
Φ	heat flow rate, heat load, power	[W]	*sh*	shading
Ψ	linear thermal transmittance	[W/(mK), W/(m°C)]	*sol*	solar
			TM	thermal bridge
			tr	transmission (heat transfer)
			use	useful
			w	wall, surface
			ve	ventilation (heat transfer)
			w	window
			ztc	thermally conditioned zone
			50	50 pascals
			∞	ambient

References

1. Veršić, Z.; Muraj, I.; Binički, M. Nearly Zero-Energy Buildings in Croatia: Comparison of Thermal Performance in Different Climatic Regions. In Proceedings of the 42nd IAHS World Congress on Housing, Napulj, Italy, 10–13 April 2018; Volume 13, pp. 16–23.
2. Prieto, A.; Knaack, U.; Auer, T.; Klein, T. Passive cooling & climate responsive façade design exploring the limits of passive cooling strategies to improve the performance of commercial buildings in warm climates. *Energy Build.* **2018**, *175*, 30–47. [CrossRef]
3. Al-Azri, N.; Zurigat, Y.H.; Al-Rawahi, N. Selection and assessment of passive cooling techniques for residential buildings in oman using a bioclimatic approach. *J. Eng. Res.* **2013**, *10*, 52–68. [CrossRef]
4. Jenkins, D.; Liu, Y.; Peacock, A.D. Climatic and internal factors affecting future UK office heating and cooling energy consumptions. *Energy Build.* **2008**, *40*, 874–881. [CrossRef]
5. European Commission, "Pv Gis." Joint Research Centre, Energy Efficiency and Renewables Unit. 2012. Available online: http://re.jrc.ec.europa.eu/pvgis/apps4/pvest.php# (accessed on 11 June 2022).
6. Bilić, T. Wind direction as one of the problems in navigation on the Adriatic in Greek and roman period. *Pomorstvo* **2012**, *26*, 81–93.
7. Rahman, M.M.; Mashud, M.; Chu, C.M.; Bin Misaran, M.S.; Sarker, M.; Kumaresen, S. A passive cooling system of residential and commercial buildings in summer or hot season. *IOP Conf. Ser. Mater. Sci. Eng.* **2015**, *100*, 012031. [CrossRef]
8. Nunes, A.I.F.; Oliveira Panão, M.J.N. Passive Cooling Load Ratio method. *Energy Build.* **2013**, *64*, 209–217. [CrossRef]
9. Brandl, H. Thermo-active ground-source structures for heating and cooling. *Procedia Eng.* **2013**, *57*, 9–18. [CrossRef]
10. Santamouris, M.; Kolokotsa, D. Passive cooling dissipation techniques for buildings and other structures: The state of the art. *Energy Build.* **2013**, *57*, 74–94. [CrossRef]
11. Ahmed, A.S.F.; Khan, K.M.M.K.; Maung Than Oo, A.A.; Maung Than Oo, A.A.; Rasul, R.M.G. Selection of suitable passive cooling strategy for a subtropical climate. *Int. J. Mech. Mater. Eng.* **2014**, *9*, 14. [CrossRef]
12. Freewan, A.A.Y. Impact of external shading devices on thermal and daylighting performance of offices in hot climate regions. *Sol. Energy* **2014**, *102*, 14–30. [CrossRef]
13. Freewan, A.A.Y. Energy-Efficient Solutions Depending on Building Forms Design with Tilted South and North Facades. *Buildings* **2022**, *12*, 753. [CrossRef]
14. Wei, L.; Tian, W.; Zuo, J.; Yang, Z.Y.; Liu, Y.; Yang, S. Effects of Building Form on Energy Use for Buildings in Cold Climate Regions. *Procedia Eng.* **2016**, *146*, 182–189. [CrossRef]
15. Premrov, M.; Žigart, M.; Žegarac Leskovar, V. Influence of the building shape on the energy performance of timber-glass buildings located in warm climatic regions. *Energy* **2018**, *149*, 496–504. [CrossRef]
16. Caruso, G.; Fantozzi, F.; Leccese, F. Optimal theoretical building form to minimize direct solar irradiation. *Sol. Energy* **2013**, *97*, 128–137. [CrossRef]
17. Hemsath, T.L.; Alagheband Bandhosseini, K. Sensitivity analysis evaluating basic building geometry's effect on energy use. *Renew. Energy* **2015**, *76*, 526–538. [CrossRef]
18. Bayoumi, M. Improving natural ventilation conditions on semi-outdoor and indoor levels in warm-humid climates. *Buildings* **2018**, *8*, 75. [CrossRef]
19. Oropeza-Perez, I. The influence of an integrated driving on the performance of different passive heating and cooling methods for buildings. *Buildings* **2019**, *9*, 224. [CrossRef]
20. Samuel, D.G.L.; Nagendra, S.M.S.; Maiya, M.P. Passive alternatives to mechanical air conditioning of building: Areview. *Build. Environ.* **2013**, *66*, 54–64. [CrossRef]
21. Breesch, H.; Bossaer, A.; Janssens, A. Passive cooling in a low-energy office building. *Sol. Energy* **2005**, *79*, 682–696. [CrossRef]
22. Kaduchová, K.; Lenhard, R. Numerical simulation of passive cooling beam and its optimization to increase the cooling power. *Processes* **2021**, *9*, 1478. [CrossRef]
23. Roulet, C.A.; Van Der Maas, J.; Flourentzou, F. A planning tool for passive cooling of buildings. *Indoor Air 96* **1996**, *96*, 265–270.
24. Roulet, C.-A.; Van der Maas, J.; Flourentzou, F. Application of Passive Convective Cooling to Buildings. Available online: https://www.researchgate.net/publication/37409999_Application_of_Passive_Convective_Cooling_to_Buildings (accessed on 12 June 2022).
25. Flourentzou, F.; van der Maas, J.; Roulet, C.-A. Experiments in Natural Ventilation for Passive Cooling. 1995, pp. 17–20. Available online: https://www.aivc.org/sites/default/files/members_area/medias/pdf/Conf/1996/Flourentzou.pdf (accessed on 12 June 2022).
26. van der Maas, J.; Roulet, C.A. Nighttime ventilation by stack effect. *ASHRAE Trans.* **1991**, *97*, 516–524.
27. Flourentzou, F.; van der Maas, J.; Roulet, C.-A. A simple model for free cooling calculations. In Proceedings of the ICSBAT '91 Conference Internationale "Energie Solaire et Batiment", Lausanne, Switzerland, 10–11 October 1991; pp. 239–245.
28. Roulet, C. Multizone Cooling Model for Calculating the Potential of Night Time; Energy Impact of Ventilation and Air Infiltration Calculating the Potential of Night Time Ventilation Authors: Jacobus Van Der Maas and Claude-Alain Roulet. January 1993. 2017. Available online: https://www.researchgate.net/publication/299600884 (accessed on 25 May 2022).
29. Pesic, N.; Calzada, J.R.; Alcojor, A.M. Assessment of advanced natural ventilation space cooling potential across Southern European coastal region. *Sustainability* **2018**, *10*, 3029. [CrossRef]

30. Zamani, Z.; Heidari, S.; Hanachi, P. Reviewing the thermal and microclimatic function of courtyards. *Renew. Sustain. Energy Rev.* **2018**, *93*, 580–595. [CrossRef]
31. Datta, G. Effect of fixed horizontal louver shading devices on thermal perfomance of building by TRNSYS simulation. *Renew. Energy* **2001**, *23*, 497–507. [CrossRef]
32. *HRN EN ISO 52016-1:2017*; Energy Performance of Buildings—Energy Needs for Heating and Cooling, Internal Temperatures and Sensible and Latent Heat Loads—Part 2: Explanation and Justification of ISO 52016-1 and ISO 52017-1 (ISO/TR 52016-2:2017; CEN ISO/TR 52016-2:2017). ISO: Geneva, Switzerland.
33. Policy, P.; Buzz, B.R.E.; Website, R.; Thermal, B.; Buzz, B.R.E.; Wiki, D.B.; Mark, H.Q.; Buzz, B.R.E.; Dengel, A.; Swainson, M.; et al. Preventing Overheating. 2020. Available online: https://www.designingbuildings.co.uk/wiki/Preventing_overheating (accessed on 25 May 2022).
34. *Tehnički Propis o Racionalnoj Uporabi Energije i Toplinskoj Zaštiti u Zgradama ((NN 128/15, 70/18, 73/18, 86/18, NN 102/20)/Technical Regulation on Rational Use of Energy and Heat Retention in Buildings (OG 128/15, 70/18, 73/18, 86/18, OG 102/20)*; Narodne Novine: Zagreb, Croatia, 2020.
35. *ANSI/ASHRAE Standard 55-2017*; Chapter 3. Building Thermal Load Estimation, 3.1 Estimation, Thermal Load Load, Heating Load, Cooling Conditions, Critical Calculations, Computer Estimation, Heating Load. American Society of Heating, Refrigerating and Air-Conditioning Engineers (ASHRAE): Atlanta, GA, USA, 2017.
36. Ahmed, K.; Kurnitski, J.; Olesen, B. Data for occupancy internal heat gain calculation in main building categories. *Data Br.* **2017**, *15*, 1030–1034. [CrossRef]
37. *Heat Gain from People, Lights, and Appliances*; Engineer Educators: New Smyrna Beach, FL, USA; pp. 1–9. Available online: https://www.scribd.com/document/523034638/engineer-educators-com-5-Heat-Gain-from-People-Lights-and-Appliances (accessed on 12 June 2022).
38. Kim, H.; Park, K.S.; Kim, H.Y.; Song, Y.H. Study on variation of internal heat gain in office buildings by chronology. *Energies* **2018**, *11*, 1013. [CrossRef]
39. *HRN EN ISO 52010-1:2017*; Energy Performance of Buildings—External climatic Conditions—Part 1: Conversion of Climatic Data for Energy Calculations (ISO 52010-1:2017; EN ISO 52010-1:2017). ISO: Geneva, Switzerland, 2017.
40. *HRN EN 1991-1-4:2012/Ispr.1:2021*; Eurocode 1: Actions on Structures—Part 1–4: General Actions—Wind Actions. Available online: https://shop.standards.ie/preview/98705226958.pdf?sku=857848_SAIG_NSAI_NSAI_204073 (accessed on 12 June 2022).
41. Gameiro, M.; Costa, J.J.; Gaspar, A.; Paulino, A.; Bento, M.; Botte, G. The Influence of Wind on the Infiltration Rates in a Web-Bases Monitored Office Building. *Roomvent* **2011**. Available online: https://www.researchgate.net/publication/260419819_The_influence_of_wind_on_the_infiltration_rate_in_a_web-based_monitored_building (accessed on 12 June 2022).
42. Kaltschmitt, M.; Streicher, W.; Wiese, A. *Renewable Energy: Technology, and Environment Economics*; Springer: Cham, Switzerland, 2007; ISBN 9783540709473.
43. Recoskie, S.; Lanteigne, E.; Gueaieb, W. A High-fidelity energy efficient path planner for unmanned airships. *Robotics* **2017**, *6*, 28. [CrossRef]
44. Etheridge, D.W. Ventilation, air quality and airtightness in buildings. In *Materials for Energy Efficiency and Thermal Comfort in Buildings*; Woodhead Publishing: Sawston, UK, 2010; pp. 77–100. Available online: https://www.sciencedirect.com/science/article/pii/B9781845695262500037 (accessed on 25 May 2022). [CrossRef]
45. *HRN EN ISO 13789:2017*; Thermal Performance of Buildings—Transmission and Ventilation Heat Transfer Coefficients—Calculation Method (ISO 13789:2017; EN ISO 13789:2017). ISO: Geneva, Switzerland, 2017.
46. Cheng, T.S. Characteristics of mixed convection heat transfer in a lid-driven square cavity with various Richardson and Prandtl numbers. *Int. J. Therm. Sci.* **2011**, *50*, 197–205. [CrossRef]
47. Santamouris, M. *Advances in Passive Cooling*; Routledge: London, UK, 2012; pp. 1–303. [CrossRef]